BIOGEOCHEMICAL GRADIENTS WITHIN AN ACID MINE DRAINAGE-DERIVED IRON MOUND, NORTH LIMA, OHIO

A Thesis

Presented to

The Graduate Faculty of The University of Akron

In Partial Fulfillment

of the Requirements for the Degree

Master of Science

Zachary J. Haake

May, 2014

BIOGEOCHEMICAL GRADIENTS WITHIN AN ACID MINE DRAINAGE-DERIVED IRON MOUND, NORTH LIMA, OHIO

Zachary J. Haake

Thesis

Approved:	Accepted:
_____	_____
Advisor Dr. John M. Senko	Dean of the College Dr. Chand K. Midha
_____	_____
Faculty Reader Dr. LaVerne M. Friberg	Dean of the Graduate School Dr. George R. Newkome
_____	_____
Faculty Reader Dr. John A. Peck	Date
_____	
Department Chair Dr. James McManus	

ABSTRACT

Acid mine drainage (AMD) is one of the most serious threats to the environment in coal mining regions. To try to determine appropriate treatment methods I evaluated the distribution of aqueous chemical species, Fe(III) minerals, and Fe- metabolizing bacteria in AMD-derived, Fe(III)-rich sediments within an AMD-impacted area of Northeast Ohio. A major goal of this work was to evaluate the depth-dependent distribution of microbially mediated redox reactions within the sediments. This research shows that aqueous Fe(II) was depleted in the sediments near the sediment-AMD interface, but increased with depth in the upper 2.5 cm of the sediments. This increase in Fe(II) concentration was likely due to Fe(III) reducing bacterial (FeRB) activities, since they were most abundant at approximately this depth interval, and poorly crystalline Fe(III) phases in the upper sediments were transformed to goethite (α-FeO(OH)) in deeper sediments, which is an indicator of FeRB activities. I also observed relatively uniform abundances of culturable Fe(II) oxidizing bacteria (FeOB) throughout the sediments, and aqueous Fe(II) was depleted below the 2.5 cm depth interval, despite minimal O_2 availability at these depths. These results indicate that while FeRB may be active in shallower regions of the sediments, FeOB remain active throughout the sediments, and may mediate transfer of electrons from deeper, O_2-depleted portions of the sediments to shallower, O_2-rich portions of the sediments.

ACKNOWLEDGEMENTS

I would not have been able to finish this thesis without the help of several people. First of all, I would like to thank my wife, Laura, for all her love and support and my baby Nathan, for giving me motivation, and also, so much love and entertainment. I would also like to thank my parents, Ron and Shirley, who encouraged me to be the best that I could be, along with my brothers, Derek and Ryan, who were accepting of me when I wasn't. Laura and my family, thank you, you have helped me more than you will ever know. Next, I would like to thank all my friends, Dave Chipps, Jim Bauman, Steve Luc, Steve Liberatore, Bobby Miller, and Jim Becker who were always ready to laugh and with your help, I was able to make it through my years here at the University of Akron. Shane Hotchkiss, who allowed me to use his work on total cell abundances. Ms. Elaine Butcher and Mr. Tom Quick, who were both incredibly knowledgeable and always happy to help. My two committee members, Dr. LaVerne Friberg, and Dr. John Peck, for their time and expertise to help me edit this thesis. Finally, my thesis advisor, Dr. John Senko. Thank you for the incredible amount of time that you spent with me, from the lab work to editing this thesis countless times. I wouldn't be where I am today without your help, thank you. This work was funded by National Science Foundation EAR Geobiology and Low Temperature Geochemistry Program award number 0851847.

TABLE OF CONTENTS

Page

LIST OF FIGURES

CHAPTER I

INTRODUCTION

Acid mine drainage (AMD) is the outflow of acidic water from surface or underground mines. This occurs naturally in some environments as part of the rock weathering process but mining and other large construction activities within rocks that contain an abundance of sulfide minerals exacerbate the problem. Upon exposure to air and water, oxidation of metal sulfides within the surrounding rock generates acidity. Bacteria and Archaea accelerate the oxidation of metal sulfides, further contributing to the development of acidic fluids. These microbes occur naturally in the rock, but limited water and oxygen supplies serve to minimize their activities (Meilke et al., 2003). The effect of AMD can be devastating to an area. When metal-rich AMD enters surface waterways, dissolved iron precipitates as an oxyhydroxide that smothers aquatic life and stains streams a rust-orange color (Lichvar, 1997). Furthermore, the acidic water coming out of the mines can lower the pH of the nearby streams, making them inhospitable for most non-microbial aquatic life (Lichvar, 1997).

Biogeochemical reactions in AMD-induced iron mounds

Biologically-mediated element cycling is directly related to electron transfer (or redox) reactions. An understanding of biogeochemical redox processes is crucial for predicting and protecting environmental health and can provide new opportunities for engineered remediation strategies. Energy necessary to sustain life can be yielded

by means of redox reactions via the oxidation of labile organic carbon or inorganic compounds (electron donors) by microorganisms coupled to the reduction of electron acceptors. Environmental redox processes play key roles in the formation and dissolution of mineral phases (Borch et al., 2009). AMD results from the microbially mediated oxidation of pyrite on exposed mineral surfaces. A general equation for AMD generation is (Banks et al., 1997):

$$2\ FeS_2 + 2\ H_2O + 7\ O_2 \rightarrow 2\ Fe^{2+} + 4\ SO_4^{2-} + 4\ H^+ \qquad \text{(Eq. 1)}$$

Sulfide mineral oxidation creates an acidic discharge that contains high levels of sulfate and dissolved metals such as Fe(II) (ferrous iron), aluminum, and manganese (Newcombe and Brennan, 2010). The dissolved metal in Appalachian coal mine drainage of greatest concern is Fe(II). The oxidation of the sulfide to sulfate and resulting acidification of fluids solubilizes the Fe(II), which upon reaching the terrestrial surface is subsequently oxidized to ferric ions (Blodau, 2006):

$$4\ Fe^{2+} + O_2 + 4\ H^+ \rightarrow 4\ Fe^{3+} + 2\ H_2O \qquad \text{(Eq. 2)}$$

Iron-rich formations are usually developed during the oxidation and hydrolysis/ precipitation of dissolved iron in the acidic solutions after they emerge from the subsurface (Espana et al., 2013).

$$Fe^{3+} + 3\ H_2O \rightarrow Fe(OH)_3 + 3\ H^+ \qquad \text{(Eq. 3)}$$

When AMD emerges and flows over the terrestrial surface with a water column height between 0.5 and 1 cm, it is considered a “sheet flow.” This “sheet-flow” characteristic

enhances the aeration of initially anoxic AMD. When the Fe(II) is oxidized, the resulting Fe(III) will hydrolyze and precipitate (Eq. 3; Martin et al., 2003). The abiotic oxidation of dissolved Fe(II) is kinetically limited in the pH range typical of coal mine-derived AMD, but aerobic acidophilic iron-oxidizing bacteria (FeOB) can mediate this reaction in these systems leading to the formation of crusts composed predominantly of Fe(III) hydroxide phases that can grow up to several meters thick and are referred to as "iron mounds" (Senko et al., 2008, 2011). As iron mound sediments accumulate, diffusion of atmospheric O_2 into the iron mound sediments may be limited, giving rise to anoxic regions of the sediment where Fe(III) reducing activity (and perhaps sulfate reducing activity) will occur, leading to the reductive dissolution of Fe(III) hydroxides, and release of soluble Fe(II) (Martin et al., 2003). Fe(II) oxidizing bacteria have to adapt to the continual burial within the iron mound as they are buried by their own waste of Fe(III) hydroxide phases that limit their oxygen supply.

Biogeochemical redox reactions in iron mounds are initiated by the activities of aerobic FeOB, which may be dependent, in part, on the vertical diffusion of O_2 within the AMD fluid and iron mound, potentially giving rise to aerobic/Fe(II)-oxidizing and anaerobic/Fe(III)-reducing zones occurring within scales of millimeters to centimeters (Meier et al., 2004). Dissimilatory sulfate-reducing bacteria reduce inorganic sulfate or other oxidized sulfur forms to sulfide. This sulfide is not incorporated into the organism but is released as "free" H_2S (Hammack et al., 2013). High concentrations of dissolved iron in ground water develop only if there is little or no sulfate reduction. This is because biogenic sulfide tends to precipitate ferrous iron as iron sulfides (Berner, 1969). Studies of anaerobic aquatic sediments have shown that sulfate reduction is largely absent if sediments contain abundant Fe(III) oxyhydroxides. Rather, sulfate reduction is only observed after Fe(III) is depleted (Froelich et al., 1979). If sufficient Fe(III) is available (as is the case in the iron mound sediments), Fe(III)-reducing microorganisms out

compete sulfate reducers and maintain concentrations of electron donors at levels that are too low for sulfate reducers to metabolize (Lovely and Phillips, 1987).

Extracellular electron transfer by microorganisms

It is becoming increasingly evident that individual microorganisms and microbial communities may exploit "charge separation" between electron donors that are spatially separated from electron donors (Nielsen et al., 2010), via processes referred to as far-afield extracellular electron transfer (EET). It is possible that microbial nanowires may influence the transfer of electrons from Fe(II) to O_2 and from organic carbon to Fe(III) phases, where microorganisms facilitate and exploit the movement of electrons from relatively reducing to relatively oxidizing regions that are spatially separated (Revil et al., 2010). Nanowires are modified pili, which may be used to establish connections to electron donors and terminal electron acceptors in anoxic conditions. Anoxic conditions will occur if the rate of oxidation of organic matter by bacteria is greater than the supply of dissolved oxygen (Nielsen et al., 2010). Iron mounds can serve as excellent models for examining far-afield extracellular electron transfer (EET) and bioelectrochemical phenomena within sediments. EET may facilitate the transfer of electrons that could otherwise not be achieved under the physiochemical conditions in immediate proximity to individual cells. Figure 1 shows a conceptual model (modified from Senko, unpublished) for how electrons may be transferred in an iron mound system, whereby electrons may be transferred from deeper, relatively reducing regions of the iron mound to shallower, relatively oxidizing regions of the iron mound via integrated networks of microorganisms, conductive microbial nanowires (or other conductive extracellular materials) and Fe(III) mineral phases. The ability of AMD-associated microorganisms to use Fe species as an electron donor or acceptor may allow them to remain metabolically

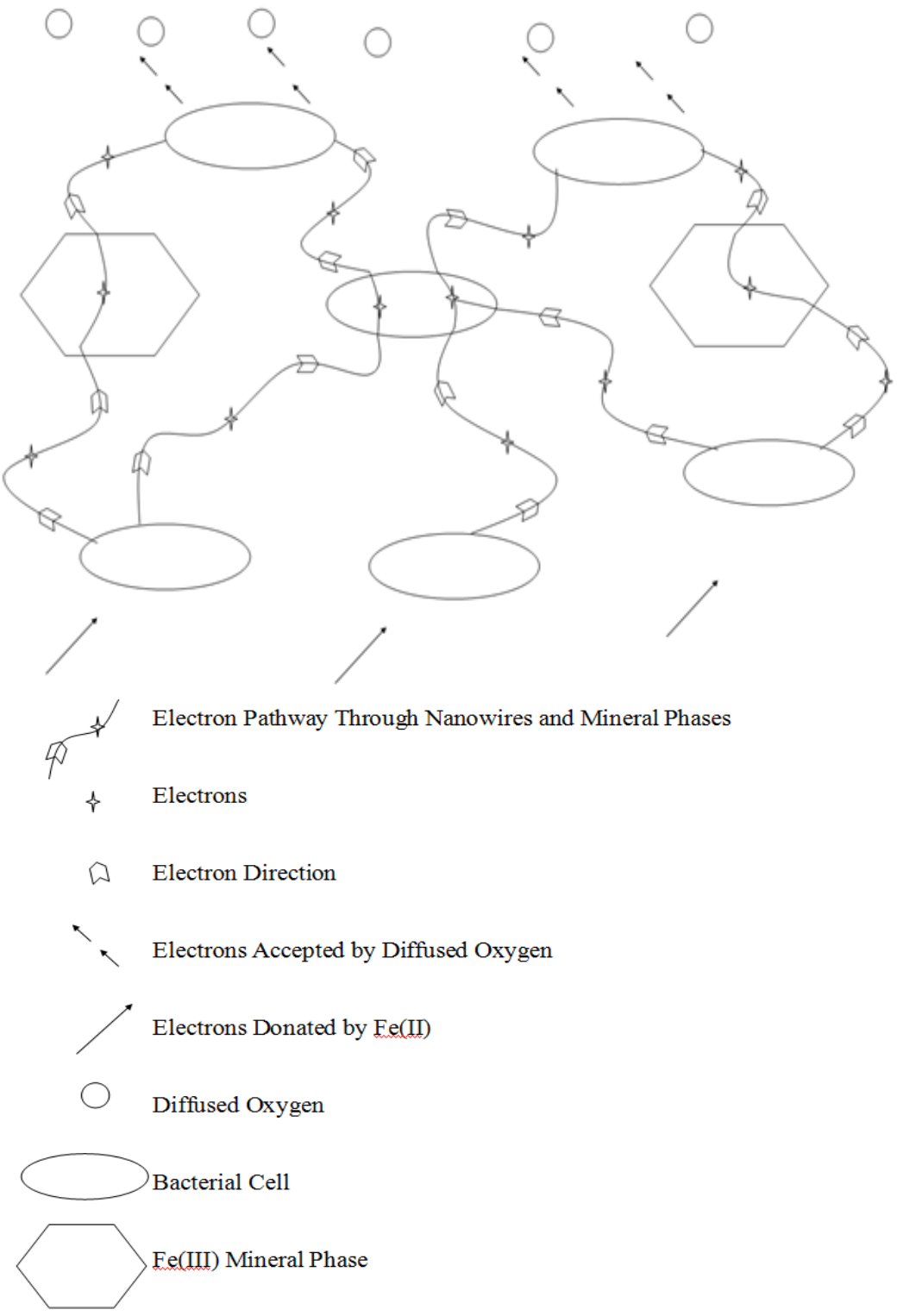

Figure 1. Electrons being transferred from Fe(II) at depth to diffused O_2 as an electron acceptor. Modified from Senko, unpublished.

active in the same spatial location despite changes in the prevailing redox conditions. Anaerobic processes are likely quite important in the overall process of EET due to the geochemical consequences of such activities. Another geochemical consequence of anaerobic versus aerobic processes in AMD-impacted systems is the formation of pH gradients, and consequent charge gradients, with aerobic Fe(II) oxidation giving rise to lower pH values, and anaerobic Fe(III) and sulfate reduction giving rise to higher pH values (Peine et al., 2000).

Hypotheses

The broad hypothesis guiding this work is that microbial communities may be integrated in iron mounds via conductive networks composed of cells, Fe-containing minerals, and microbial nanowires that allow oxidation to occur at depth within the iron mound (Fig. 1). I hypothesize that vertical geochemical and mineralogical gradients should be evident within the iron mound, and are indicative of microbiological activities. If Fe(II) concentrations within the iron mound decrease at varying depths it indicates that there are oxidizing zones. If there is a decrease in sulfate concentration, then Fe(II) concentrations should increase concurrently, which is suggestive of anaerobic activities. If distributions of FeRB and FeOB are dependent just on vertical diffusion of O_2 within the sediments, I would expect to see more FeOB on top and more FeRB at depth. If "far afield" electron transfer occurs, I would expect to see a uniform distribution of FeOB and FeRB.

Approach

The vertical distributions of aqueous chemical species, Fe(III) phases, FeOB, and iron-reducing bacteria (FeRB) must be established in order to evaluate the dynamics of electron transfer in the iron mounds. I determined depth-dependent gradients within the iron mound by characterization of material I collected from iron mound cores. I evaluated the aqueous chemistry at various depths within the iron mound sediments as well as abundances of FeOB and FeRB using culture-dependent approaches. By understanding the prevailing chemical conditions, iron mineralogy, and distributions of FeOB and FeRB, I was able to predict the dynamics of the flow of electrons in the iron mound, and determine if Fe(II) oxidation occurs exclusively at the surface or at depth within the iron mound.

CHAPTER II

METHODS

The AMD-impacted site examined in this study is located in North Lima, Mahoning County, Ohio and is referred to as the Mushroom Farm (Figure 2). A house on the property roughly sits atop an abandoned underground coal mine, and land surrounding the Mushroom Farm was more recently disturbed due to surface mining activities to exploit the same coal seam that was excavated during underground mining activities (Cheryl Socotch, personal communication). A mushroom farm is set to the side of the property where mushrooms were cultivated until the early 1990's. After mushroom farming stopped, AMD seeps developed throughout the property. The AMD filled the basement of the house and began seeping out of the window well into the surrounding yard (Figure 3).

AMD with pH 4.5 and a Fe(II) concentration of 12 mM flows downhill as a 0.5 -1 cm sheet and oxidation of Fe(II) in the AMD has led to the development of an iron mound that covers an area of approximately 45 m (Gouin et al., 2012). As the AMD flows over the terrestrial surface FeOB activities lead to the removal of >90% of the dissolved Fe(II) over a distance of 30 m, via the oxidation of Fe(II), and subsequent hydrolysis of biogenic Fe(III) (Gouin et al., 2012). The iron mound is covered in a sheet flow throughout the year, which prevents it from drying out and contracting during the dry season. Similarly, freezing of the AMD in the study region of the iron mound has only been once (winter 2014) in the period spanning 2009 to 2014 (Senko, personal communication). At a portion of the iron mound that is approximately 6 m

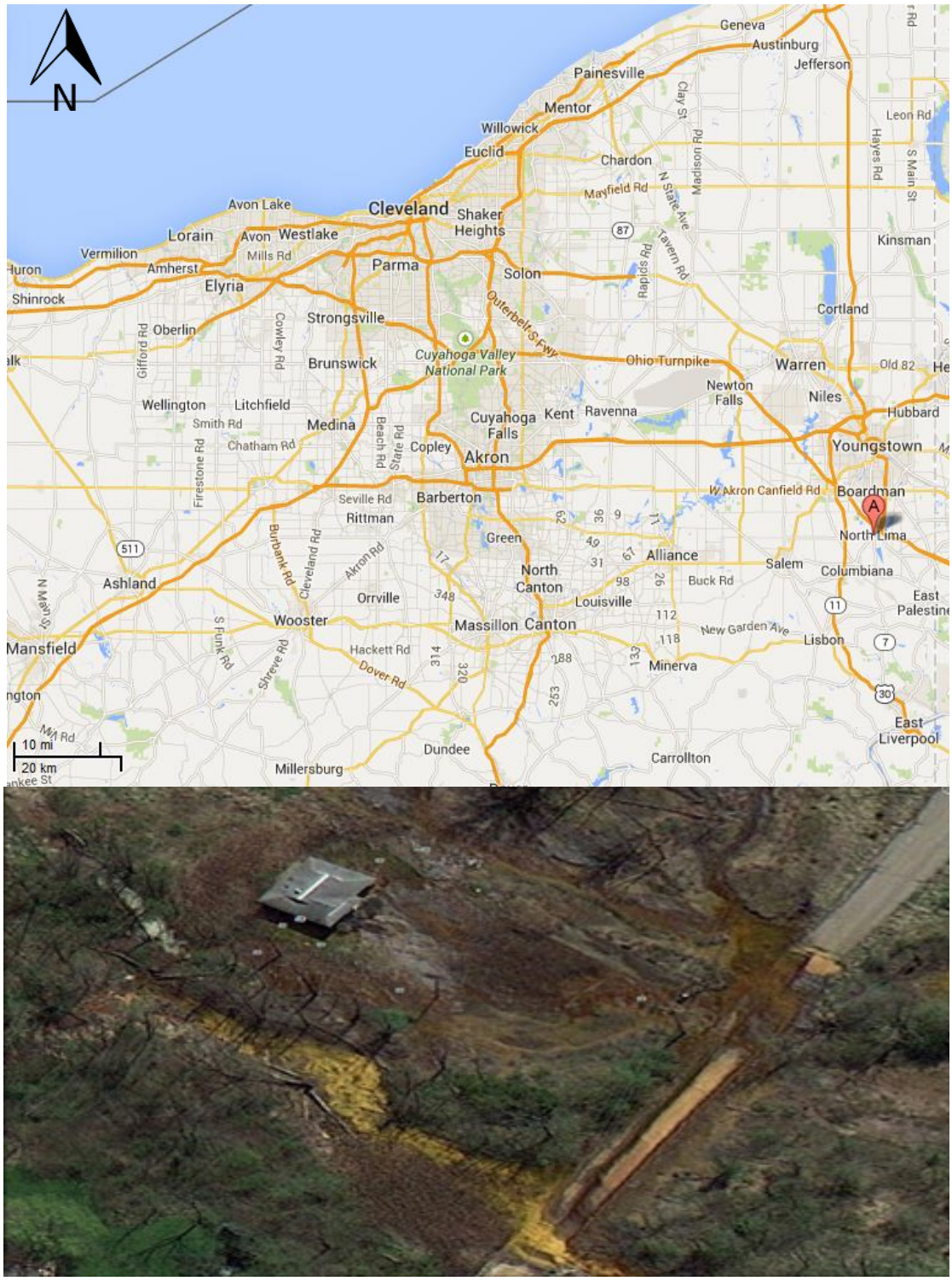

Figure 2. A location map of North Lima along with an aerial view of the Mushroom Farm.

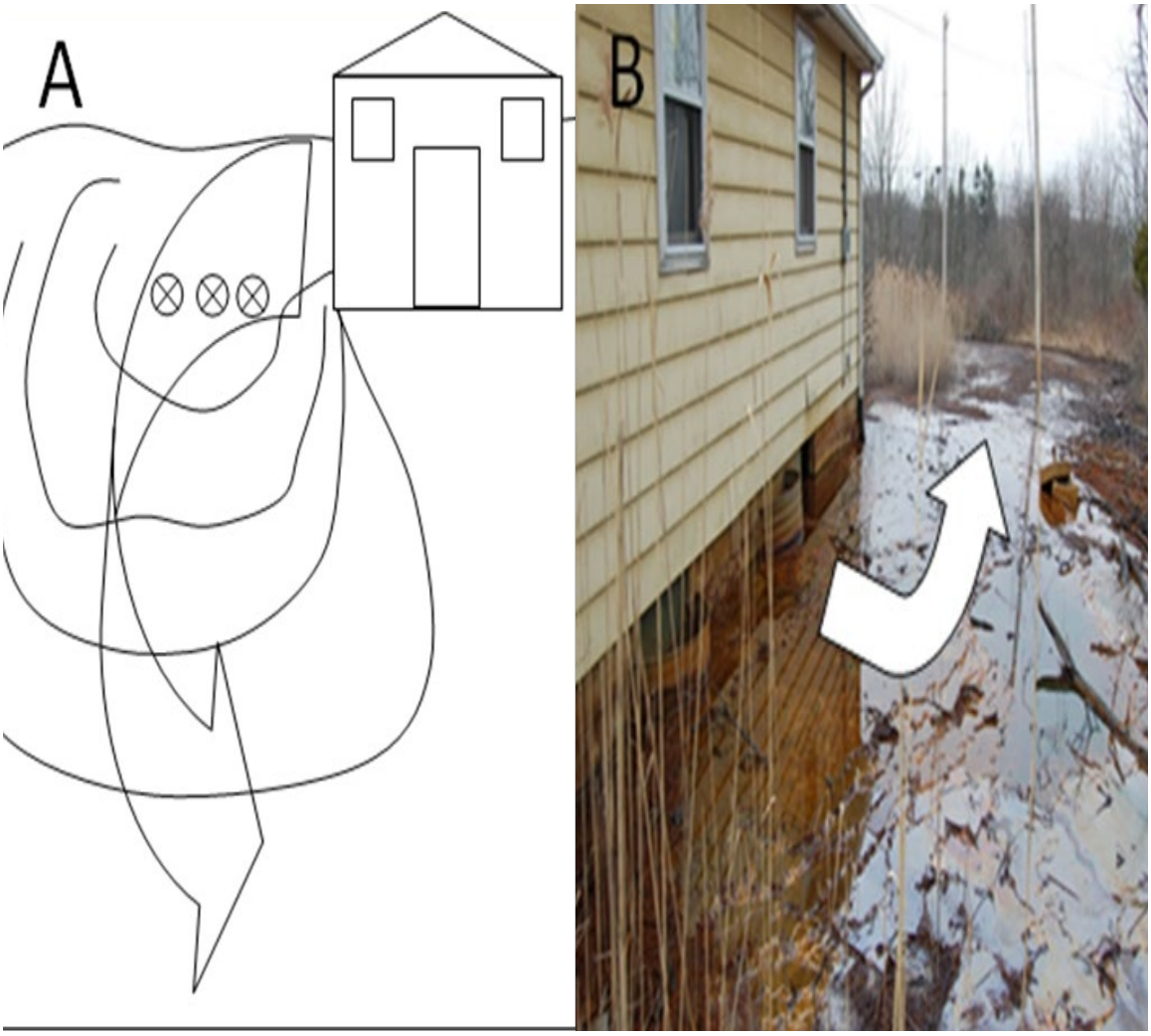

Figure 3. Schematic depiction (A) and site photograph (B) of the Mushroom Farm iron mound. The schematic view shows that the iron mound developed to the left side of the house as it formed a terraced crust composed predominantly of Fe(III) hydroxide phases. The arrow indicates the direction of the AMD as it flows down the iron mound. I collected samples at the top of the mound, close to the emergence point of the AMD from the house. The sampling region is depicted by ⊗ in panel A. The site photograph has a viewpoint from the top of the iron mound looking down it. This is also the emergence point of the AMD as it seeps out the side of the basement and runs downhill in the direction of the arrow.

from the AMD emergence point, Fe(III) hydroxides have accumulated to a thickness of approximately 10 cm. AMD has been flowing in this fashion for 20 years, indicating an iron mound "growth" rate of 0.5 cm/yr. The pH of water flowing over the iron mound ranges from 2.5 – 4.5.

Core Collection

I collected cores from a 0.5 m^2 portion of the Mushroom Farm iron mound located approximately 6 m from the AMD emergence point using 60 cc syringes with the luer end removed. Each core was cut into 10 segments at 1 cm intervals to determine pH at each depth within the iron mound. These cores are roughly 10 cm in length and provided samples of the entire depth sequence of the iron mound crust. Recovered cores were covered with plastic wrap, sealed with vinyl tape, and placed on ice for transport to the laboratory. Cores used for culture-dependent microbial enumerations were collected in the same fashion, but the syringes were autoclaved and cores were stored at 4^{o}C for no more than one week before enumerations were initiated (described below). Sediment was extruded from the core at 1 cm increments with the sediment-water interface as the starting point of measurements, and pH was determined by mixing 2 g of wet iron mound material from each depth interval with 4 mL of ultrapure water. This mixture was vortexed and pH was measured using a VWR, symphony B10P, benchtop pH meter. A total of six cores were collected at 2 cm depth intervals to determine the mineralogy of sediment at different depths by powder X-Ray diffraction (XRD) using a Phillips 3100 automated diffractometer using a CuKα radiation, and scanning at 2Θ of 2^{o} to 70^{o} with accelerating voltage of 40kV at 35 mA. X-Ray intensities were determined with 0.02^{o} step size and 1 sec counting time/step. Two cm depth intervals were evaluated by XRD to allow sufficient material for XRD sample holders. Mineral identification

was accomplished by comparing reference pattern in the measured pattern against the Cambridge Structural Database (CSD) (Groom et al., 2011).

Passive Sampler Deployment

After the sediment cores were removed, passive sampling devices similar to those described by Spalding and Brooks (2005) were deployed into the holes left by the cores. The passive sampler devices (referred to as agarose "plugs") were composed of solidified agarose (5% in 1mM KBr-amended deionized water) cylinders that could be used to provide depth-dependent geochemical information at a much finer scale than what could be obtained from analyzing core material alone. Agarose forms in an inert matrix utilized in separation techniques. Agarose plugs were used to determine iron and sulfate at depths within the iron mound at 0.5 cm increments. The plugs used the agarose as a solidifying agent and they also contain KBr to assure that the plug has equilibrated with the surrounding AMD. The plugs were recovered after six months of incubation in the iron mound, after which, they had swelled to fill the void left behind by coring.

Cores were transported back to the laboratory, and each plug was sectioned at 0.5 cm intervals. Sections were then cut in half, with one half of the section immersed in HCl and the other half immersed in nanopure water. Both sections were macerated, and incubated for 24 hr. Solids were separated from the fluid by centrifugation, and Fe(II) (in HCl-incubated plug section) and sulfate and bromide (in water-incubated plug sections) were quantified. Dissolved Fe(II) was quantified by ferrozine assay (Stookey, 1970), and sulfate and bromide were quantified by ion chromatography using a Dionex DX-120 system fitted with an AS4A column and conductivity detector (Dionex, Sunnyvale, CA). Complete equilibration of the plug-associated fluid with the surrounding iron mound pore-water was achieved, as I was unable to detect bromide in any of the plug

sections. To assure that Br^- could be detected in agarose plugs, a plug was cast with Br^- and processed as described above. Complete recovery of Br^- was observed after this extraction step.

Culture-dependent Microbial Enumerations

FeRB and FeOB were enumerated in sediments recovered from cores at a resolution of 1 cm, using culture-dependent approaches. To enumerate FeRB, extruded core material was transferred to an anoxic glovebag (Coy Laboratory Products, Grass Lake, MI), and sediment was suspended in a medium that contained 10 mM $(NH_4)_2SO_4$, 2 mM $MgSO_4$, 25 mM $Fe_2(SO_4)_3$, 5 mM glucose, 0.5 g/l trypticase soy broth (TSB), vitamins and trace metals, with a pH adjusted to 4.2 with NaOH (Senko et al., 2009). These sediment suspensions in medium were serially diluted in a three-tube most probable number (MPN) dilution series (Colwell, 1979). Cultures were incubated in the dark room temperature and scored after 6 weeks incubation based on the accumulation of > 4 mM Fe(II) in the cultures. Aerobic FeOB were enumerated by a plate-counting approach using a medium described by Johnson (1995). This solid medium contained 25 mM $FeSO_4$, 14 mM $(NH_4)_2SO_4$, 2mM $MgSO_4$, 0.25 g/l trypticase soy broth, vitamins and trace metals (Tanner, 1997). Core material was suspended in a solution that contained 14 mM $(NH_4)_2SO_4$ and 2 mM $MgSO_4$ (pH adjusted to 3.5 with H_2SO_4), and this suspension was serially diluted in the same solution. Dilution series from each depth interval were subsequently spread onto the solid medium described above, incubated in the dark at room temperature, and FeOB colony forming units (CFU) were counted based on the formation of colonies that were encrusted in red Fe(III) hydroxide precipitates.

CHAPTER III

RESULTS

The focus of this work was to determine the depth-dependent dynamics and distribution of Fe-metabolizing microbial activities. To get a better understanding of these processes, I evaluated geochemical (pH, Fe(II) and sulfate concentrations), mineralogical, and microbial (FeRB and FeOB) gradients, at depth within the MF iron mound.

A geochemical consequence of anaerobic versus aerobic processes in AMD-impacted systems is the formation of pH gradients, with aerobic Fe(II) oxidation giving rise to lower pH values (reaction 1) and anaerobic Fe(III) reduction giving rise to higher pH values (reaction 2) (Peine, 2000; Senko et al., 2010).

$$4Fe^{2+} + O_2 + 4H^+ \rightarrow 4Fe^{3+} + 2H_2O \qquad \text{(reaction 1)}$$

$$Fe^{3+} + 3H_2O \rightarrow Fe(OH)_3 + 3H^+ \qquad \text{(reaction 2)}$$

In the same way, I hypothesized that there should be vertical geochemical gradients within the iron mound, with relatively low Fe(II) concentrations suggestive of oxidizing zones, and relatively high Fe(II) concentrations suggestive of anaerobic activities. Similarly, if there is a decrease in sulfate concentration it is suggestive of anaerobic activities. Mineralogical gradients within the iron mound may also be indicative of in situ microbial activities (Brantner et al., submitted).

There should be vertical mineralogical gradients within the iron mound that accompany anaerobic microbial activities. The Fe(III) mineral phases will change with depth as poorly crystalline Fe(III) phases (including hydrous ferric oxide, ferrihydrite, schwertmannite) transforms into goethite. If distribution of FeRB and FeOB are dependent only on vertical diffusion of O_2 within the sediments, I would expect to see more FeOB on top and more FeRB at depth, and therefore a lower pH at the top and a higher pH at depth.

Depth-dependent geochemistry

Sediment pH was 3.04 close to the surface of the iron mound sediments (Figure 4). As the depth increased, the pH value decreased. The lowest pH value was at 5 cm with a pH of 2.74. There was a slight increase in pH as the depth increased from 5-10 cm with a pH of 2.82 at 10 cm, but the pH value stabilized at a depth below 4 cm. Using passive sampling agarose plugs, I measured pore-water Fe(II) and sulfate concentrations at 0.5 cm intervals from the iron mound surface to a depth of 9 cm. Two agarose plugs were removed after three months of incubation in the field. The plugs used agarose as a solidifying agent and also contain KBr to assure that the plug equilibrated with the surrounding AMD. It was determined that the plugs had equilibrated sufficiently since KBr was not detected in the plugs after they had been incubated in the field. These two plugs were used to determine the sulfate and Fe(II) concentrations at depth.

The pore-water, Fe(II) average of the two plugs had an initial concentration of 3.39 mM just below the sediment-water interface. The lower initial Fe(II) concentration at the top is likely because that is where Fe(II) oxidation is occurring due to readily available dissolved O_2 close to the sediment-water interface (Figure 4). Fe(II) concentration increased to 6.71 mM at 2.5 cm, most likely due to Fe(III) reduction. Fe(II) then

decreased with depth, possibly from Fe(II) oxidizing zone that is roughly 3 cm from the surface or adsorption of Fe(II) onto Fe(III) hydroxide phases in the iron mound (Figure 4). The Fe(II) concentration slowly decreased between 3-8 cm with a final Fe(II) concentration of 2.76 mM at 8 cm, but after 4.5 cm there was very little change in the Fe(II) concentration. The Fe(II) concentrations peaked around 3 cm, with lower concentrations at the top and bottom of the iron mound plug, suggesting that there would be more Fe(II) oxidation at these locations.

The pore-water sulfate within the plugs had an initial concentration of 127 mM at the top of the iron mound (Figure 4). From this point there was a decrease in concentration to 86 mM by 2.5 cm. After that depth, the sulfate concentration generally stabilized at a concentration of approximately 80 mM throughout the remainder of the iron mound (Figure 4).

Depth-dependent mineralogy

The MF iron mound cores were sectioned at 2 cm depth intervals and then dried in an anoxic environment for mineralogical analysis of the iron mound material at different depths (Figure 5). Samples from discrete depths within the iron mound were analyzed by XRD to identify the mineralogy of Fe(III) phases in the iron mound. Analysis of the solid phases in the upper 2 cm of the iron mound by XRD showed poorly resolved peaks, indicative of poorly crystalline Fe(III) phases, which may include hydrous ferric oxide, ferrihydrite, or schwertmannite, which is a poorly ordered Fe(III) hydroxysulfate that is commonly encountered in AMD-impacted systems (Bingham et al, 1990, 1994). It is possible that the upper surface layer is a combination of schwertmannite and disorganized goethite. As the depth increased on each core, the XRD pattern contained sharper, more defined peaks, with higher peak to background ratios, suggesting that these phases were

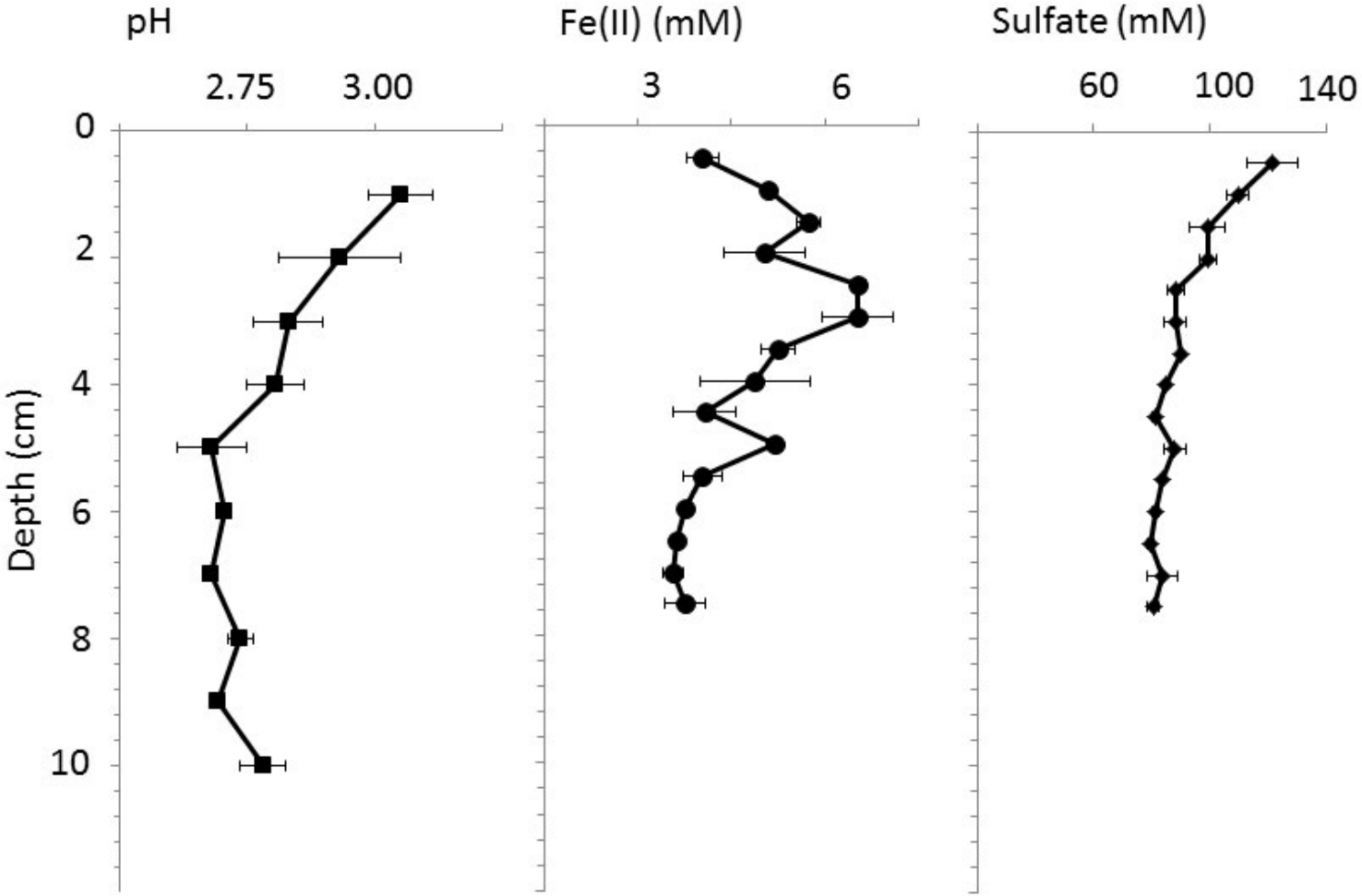

Figure 4. pH of sediment-water suspensions of material recovered from various depths. Pore-water Fe(II) and sulfate concentrations at various depths in a passive sampling agarose plug deployed in the iron mound at the MF. Error bars represent standard deviations of measurements obtained from duplicate passive sampling agarose plugs.

more crystalline in comparison with the top of each core. The predominant mineral phases in deeper regions of the cores were identified by XRD as goethite, indicating that there was a post-Fe(III) phase deposition transformation of poorly crystalline phases to a more crystalline form of goethite. This transformation can be attributed to the onset of anoxic conditions and consequent bacterially-mediated reduction of poorly crystalline Fe(III) phases (Hansel et al., 2003; Burton et al., 2008). I collected a total of six cores from the field to produce profiles by XRD. Each core was in a line and was collected approximately 6 inches from one another. Depth-dependent mineral signatures in all of these cores were almost identical (Figures 5-10), illustrating that there is mineralogical homogeneity within the approximately 0.5 m^2 area of the iron mound that was sampled.

Depth-dependent distributions of microorganisms

FeRB and FeOB were enumerated in sediments recovered from cores at a resolution of 1 cm, using culture-dependent approaches. FeRB were enumerated using a most probable number (MPN) series in aSRBFe medium (Senko et al., 2009). Aerobic FeOB were enumerated by a plate-counting approach using medium described by Johnson (1995).

FeOB were most abundant in the shallowest sediments, likely due to increased amount of diffused O_2, and then decreased slightly with depth (Figure 11). However, they remained abundant throughout the sediment, despite evidence of anaerobic activities in deeper portions of the iron mound. At the bottom of the core, the colony forming units increased to more than the initial amount at the top of the core, so that for the FeOB there is a uniform distribution, and surprisingly high number of FeOB in the deepest sampled region of the iron mound. From the top of the sediment, the FeRB had an opposite pattern of the FeOB with an initial increase in abundance, with the maximum

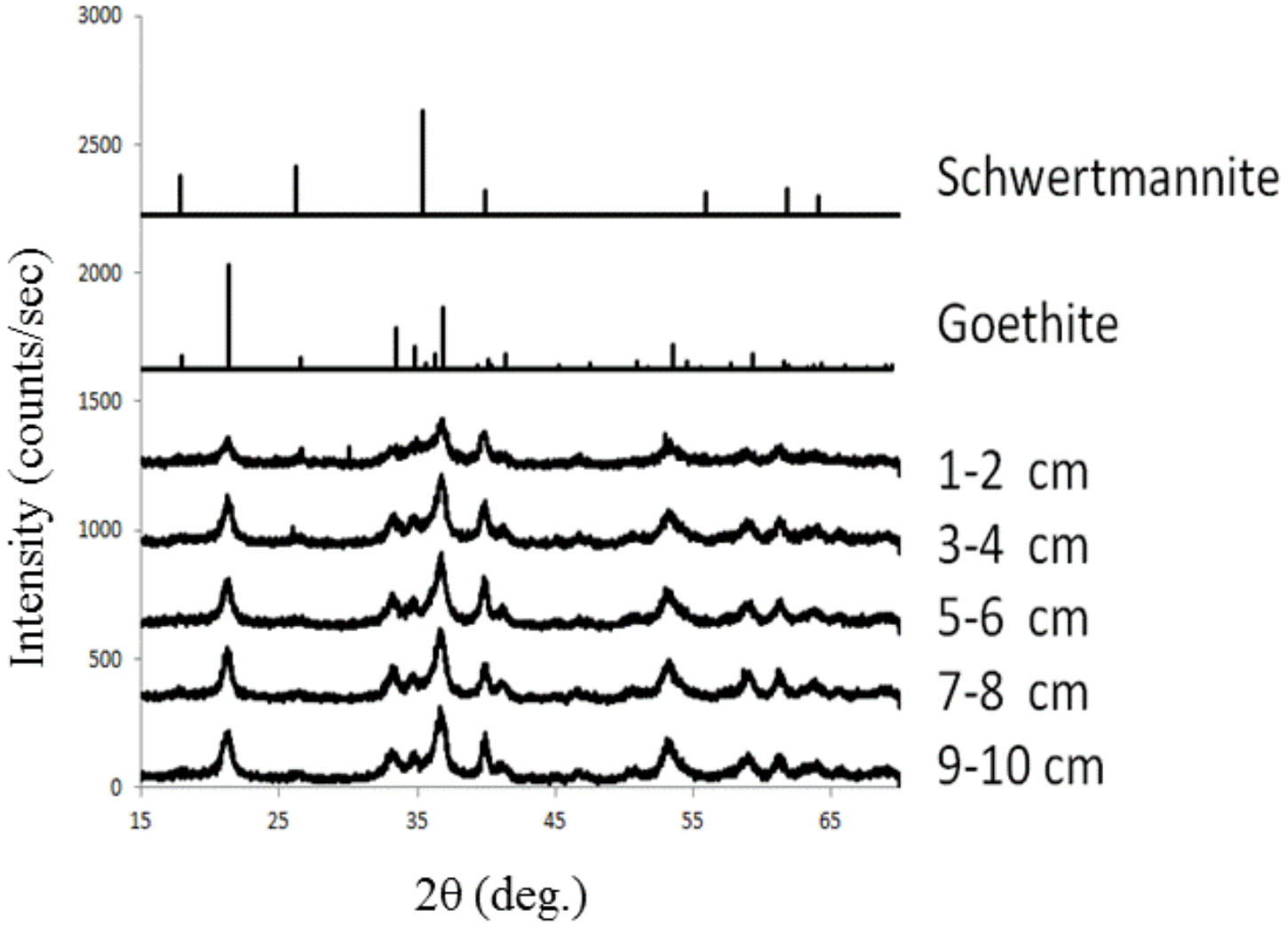

Figure 5. XRD patterns obtained from sediments (of Core 1) at various depths within the iron mound. Reference patterns of goethite and schwertmannite are from the American Mineralogist Crystal Structure Database (Downs et al., 2003). Reference patterns are plotted using a scale of relative intensity. Samples are offset to allow visualization of individual patterns.

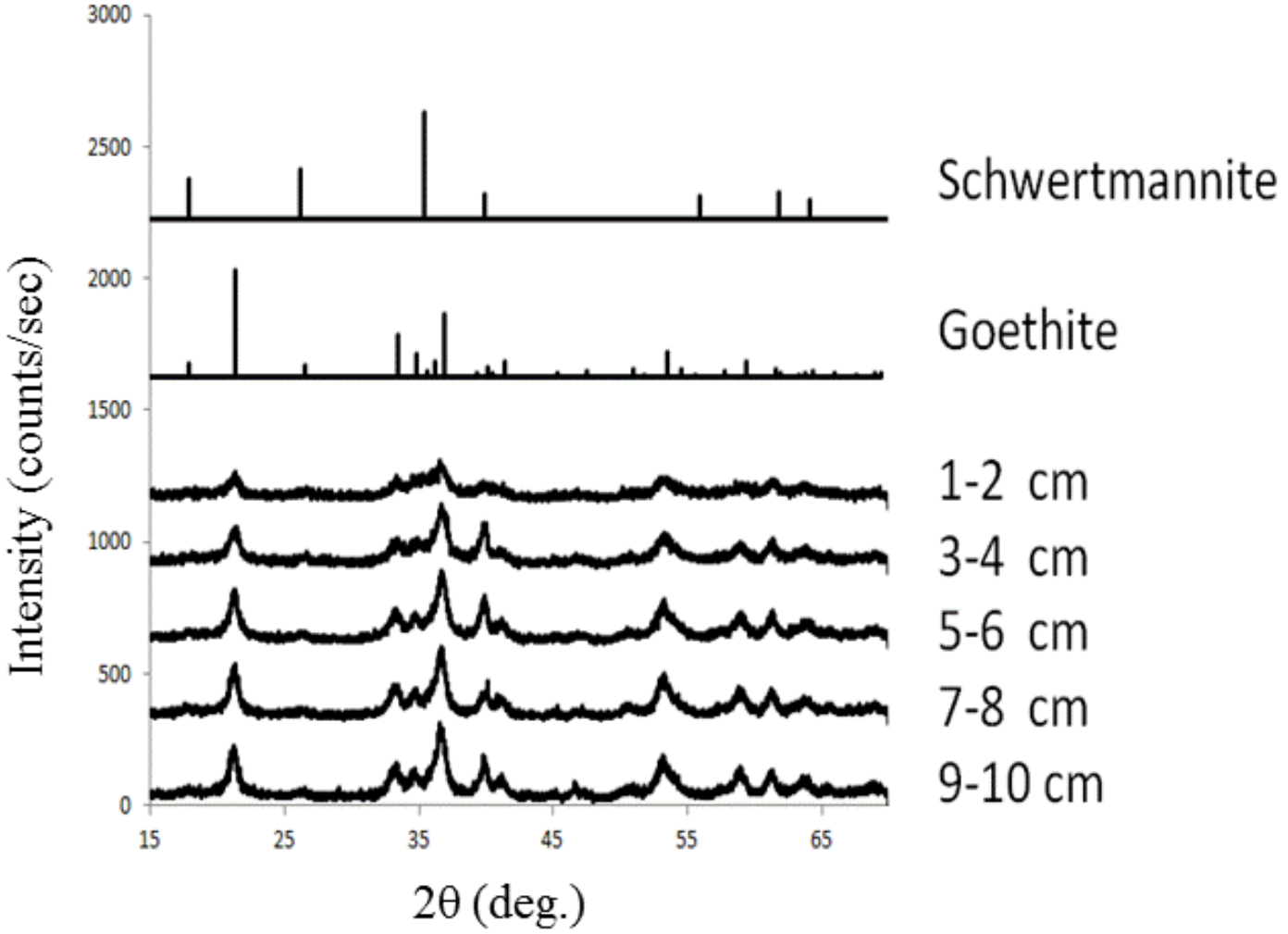

Figure 6. XRD patterns obtained from sediments (of Core 2) at various depths within the iron mound. Reference patterns of goethite and schwertmannite are from the American Mineralogist Crystal Structure Database (Downs et al., 2003). Reference patterns are plotted using a scale of relative intensity. Samples are offset to allow visualization of individual patterns.

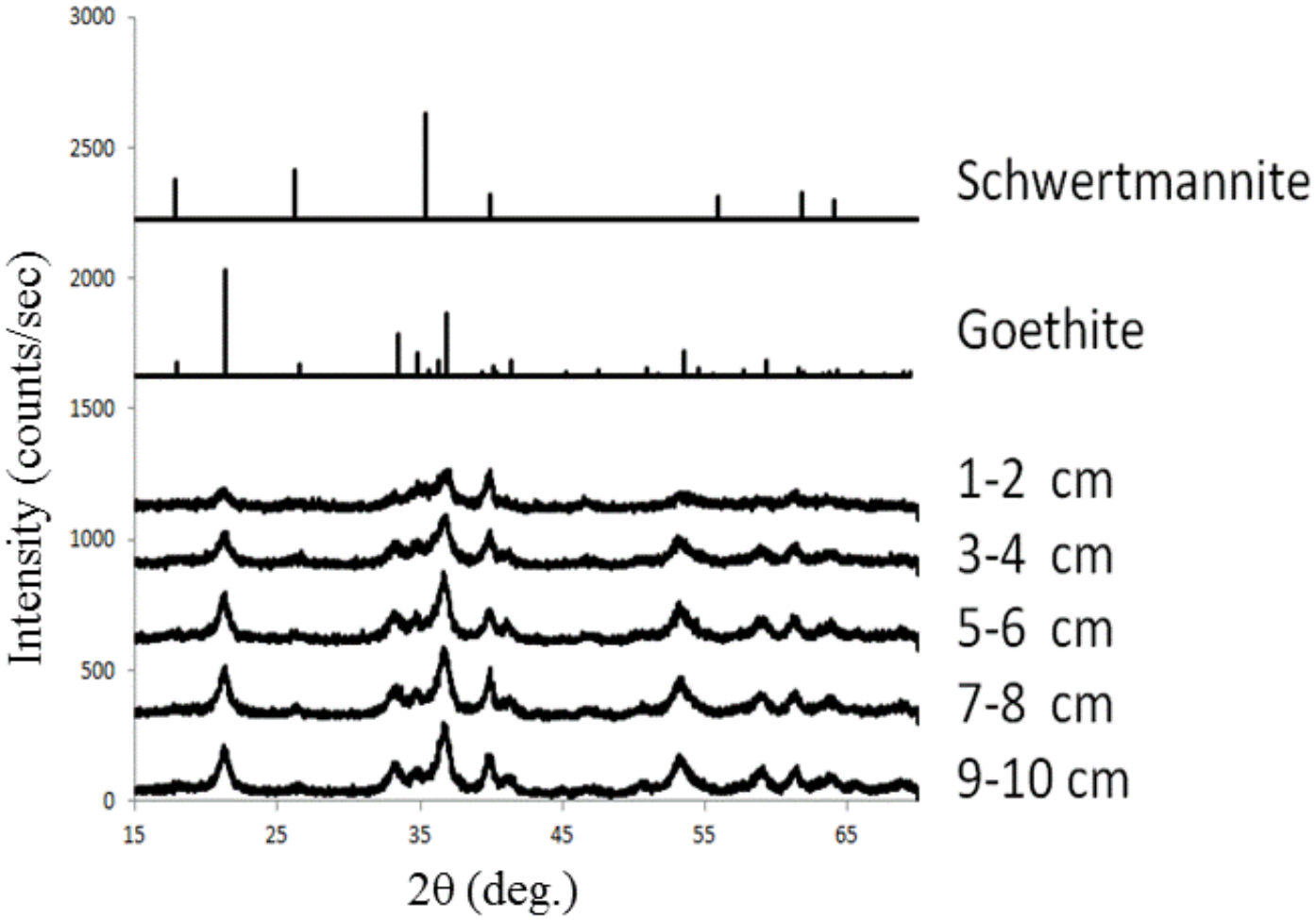

Figure 7. XRD patterns obtained from sediments (of Core 3) at various depths within the iron mound. Reference patterns of goethite and schwertmannite are from the American Mineralogist Crystal Structure Database (Downs et al., 2003). Reference patterns are plotted using a scale of relative intensity. Samples are offset to allow visualization of individual patterns.

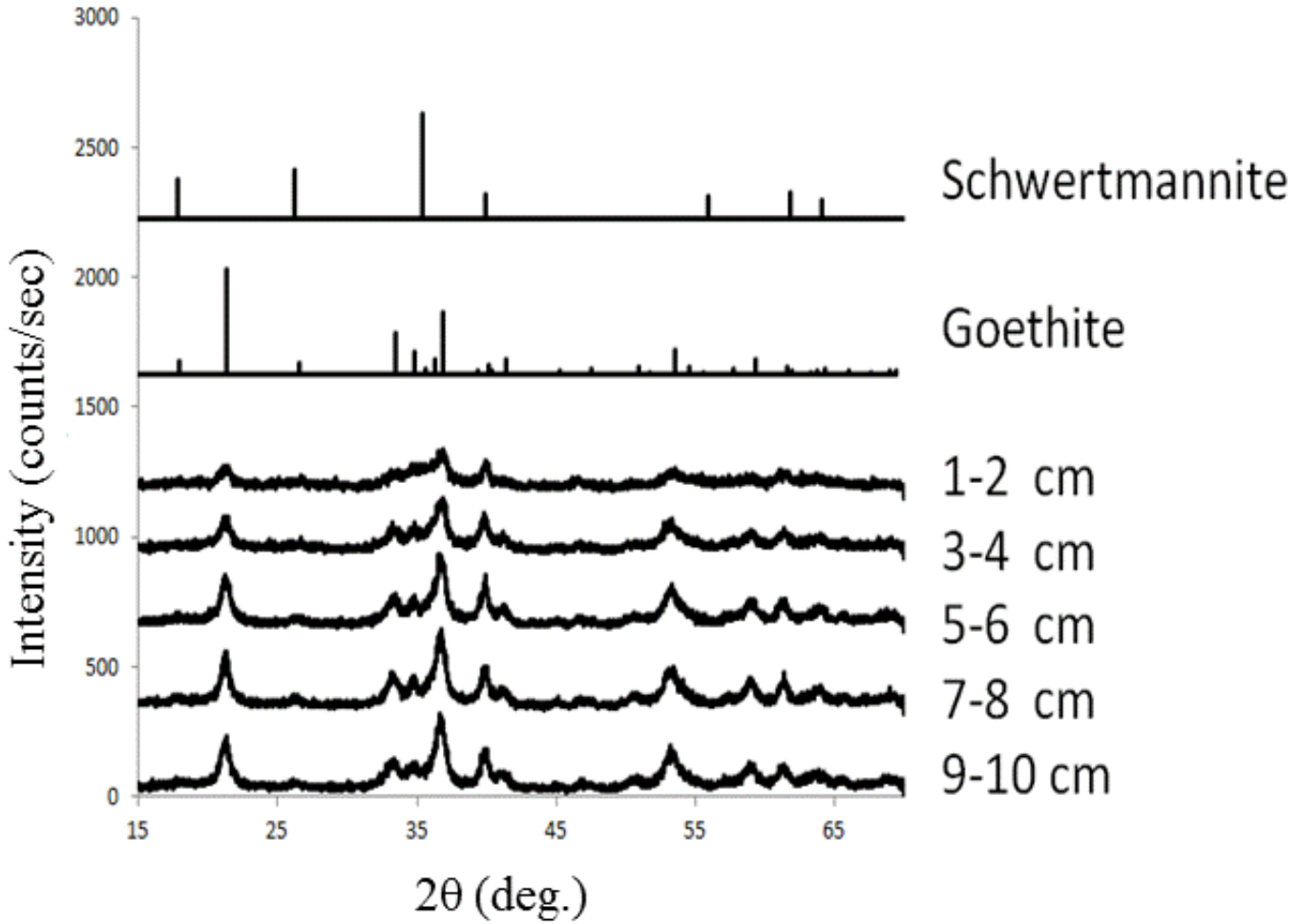

Figure 8. XRD patterns obtained from sediments (of Core 4) at various depths within the iron mound. Reference patterns of goethite and schwertmannite are from the American Mineralogist Crystal Structure Database (Downs et al., 2003). Reference patterns are plotted using a scale of relative intensity. Samples are offset to allow visualization of individual patterns.

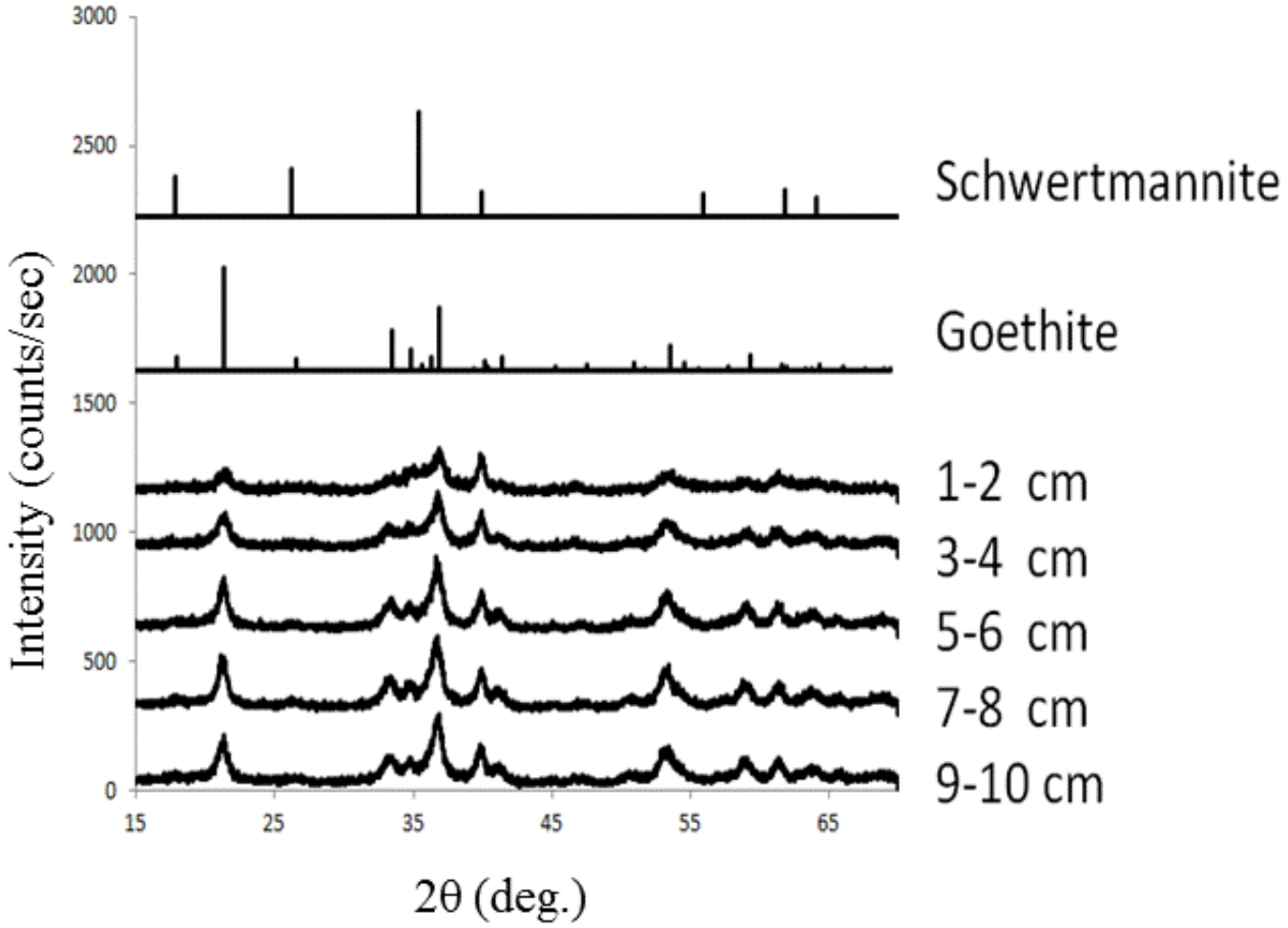

Figure 9. XRD patterns obtained from sediments (of Core 5) at various depths within the iron mound. Reference patterns of goethite and schwertmannite are from the American Mineralogist Crystal Structure Database (Downs et al., 2003). Reference patterns are plotted using a scale of relative intensity. Samples are offset to allow visualization of individual patterns.

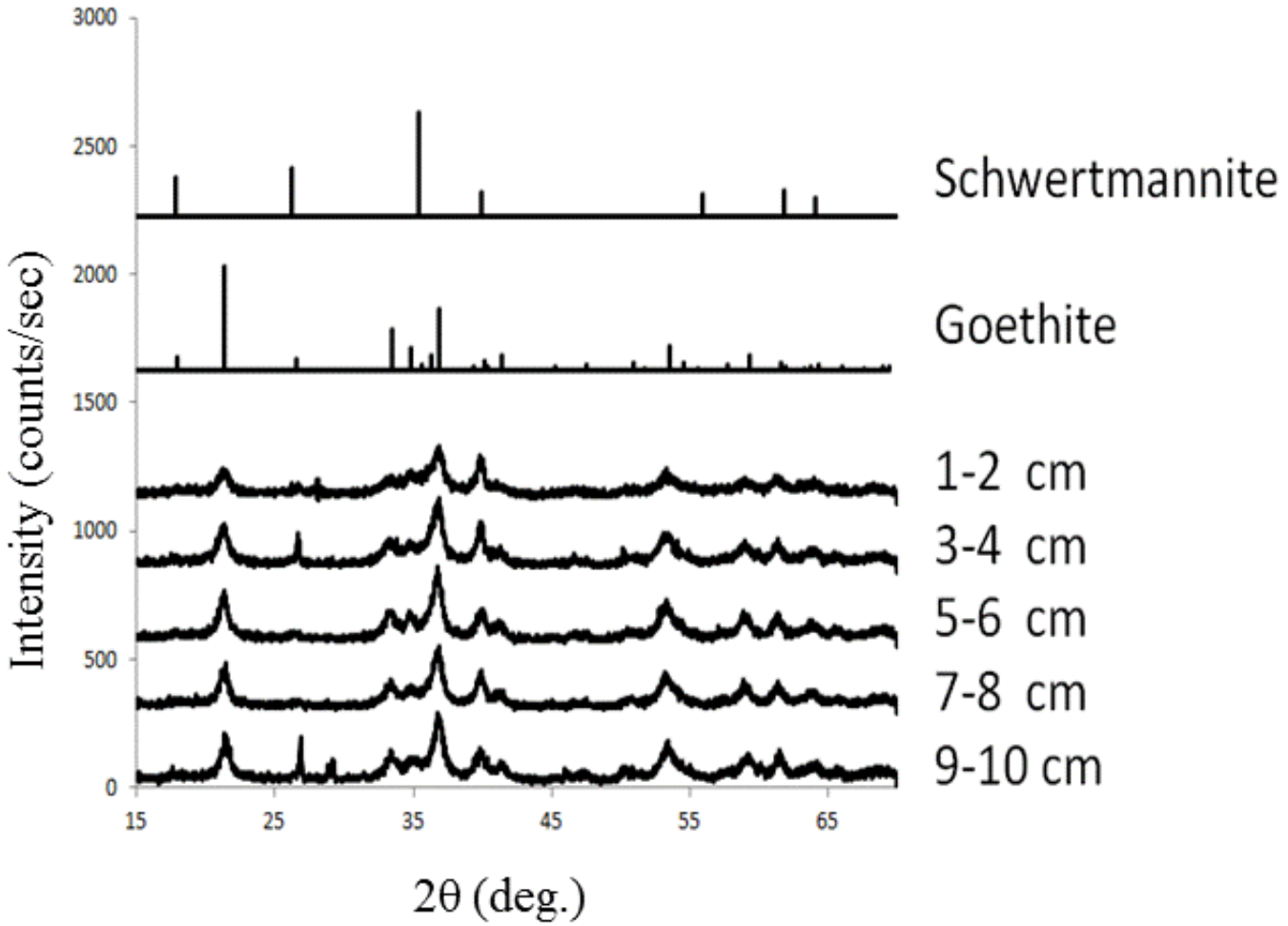

Figure 10. XRD patterns obtained from sediments (of Core 6) at various depths within the iron mound. Reference patterns of goethite and schwertmannite are from the American Mineralogist Crystal Structure Database (Downs et al., 2003). Reference patterns are plotted using a scale of relative intensity. Samples are offset to allow visualization of individual patterns.

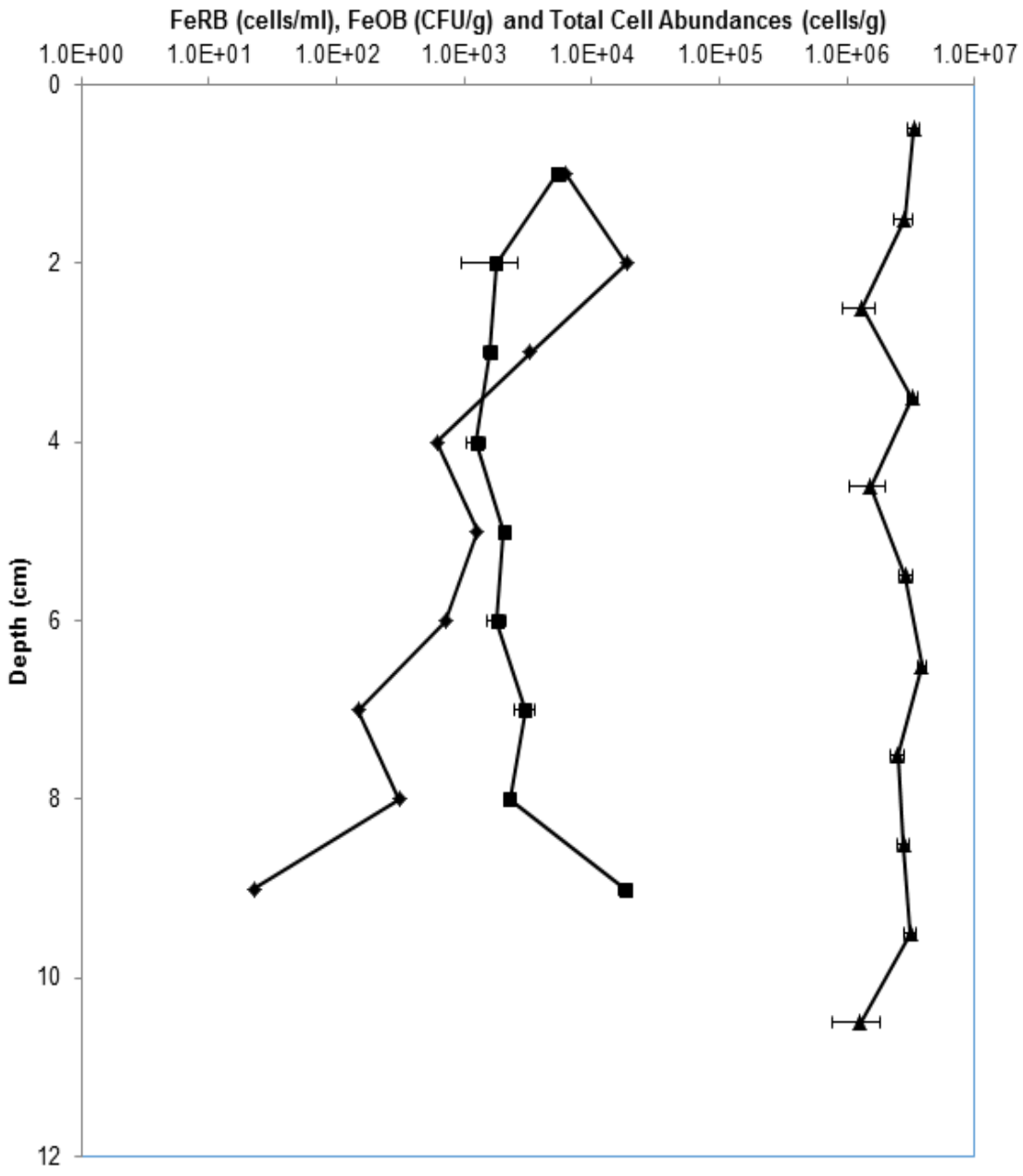

Figure 11. Abundances of (♦) FeRB, (■) FeOB, and (▲) total cell abundances at the MF iron mound as depth increases. Error bars represent standard deviations measurements obtained from duplicate FeOB plate-counting approaches and total cell counts. Total cell counts are courtesy of Shane Hotchkiss.

amount at 2 cm (Figure 11). FeRB abundance then decreased with greater depth through the sediment (Figure 11). The total cell abundances were constant throughout the core (Figure 11). These cell abundances were larger than the sum of FeOB and FeRB abundances (accounting for less than 0.5% of total cell abundances), suggesting that non-Fe-metabolizing organisms are abundant in the iron mound sediments or that the culture-dependent approach that I used was insufficient to recover all types of Fe-metabolizing organisms. Nevertheless, it appears that FeOB were distributed uniformly throughout the sediments, while cultureable FeRB appeared to be most abundant in the shallower regions in the iron mound.

CHAPTER IV

DISCUSSION

A conceptual model of potential distributions of microbiological activities (and geochemical consequences of these activities) is shown in Figure 12. The most abundant terminal electron acceptors in the MF iron mound system are oxygen, Fe(III) and sulfate. In any given location, as the most energetically favorable electron acceptor is depleted, the microbial community will adapt to take advantage of the next most thermodynamically favorable electron acceptor available (Champ et al., 1979; Froelich et al., 1979; Lyngkilde and Christensen, 1992; Lovley and Chapelle, 1995; Anderson and Lovley, 1997; Christensen et al., 2000; Coates and Achenbach, 2001).

A major controller of microbial activities in this system will be atmospheric O_2 which diffuses at the sediment-water interface. Because of this, our conceptual model of the distributions of microbial activities predicts that aerobic Fe(II) oxidizing activity would occur only toward the surface, leaving Fe(III) and sulfate reduction to occur in deeper O_2-depleted regions. Diffusion of O_2 at the sediment-water interface would create low Fe(II) concentrations at the surface that would increase with depth and O_2 depletion, and sulfate concentrations that decrease slightly initially from the surface and then more significantly with greater depth (Figure 13). A geochemical consequence of anaerobic versus aerobic processes in AMD-impacted systems is the formation of pH gradients. Aerobic Fe(II) oxidation give rise to lower pH values (equation 4), and anaerobic processes (Fe(III) and sulfate reduction) (equations 5 and 6) give rise to higher pH values (Peine et al., 2000; Senko et al., 2009). Therefore, pH would then decrease sharply at the sediment-water

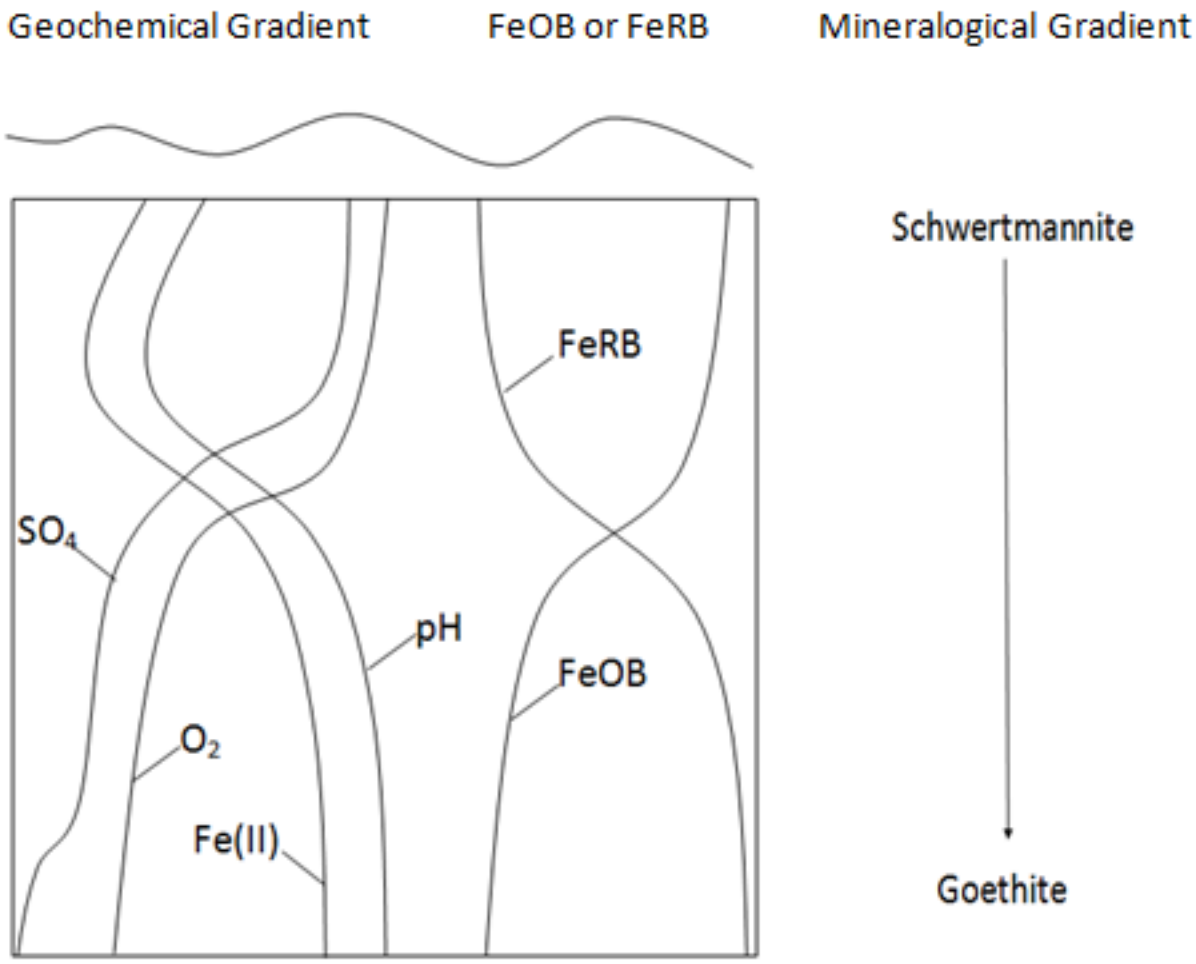

Figure 12. Conceptual model of the distributions of microbial activities and geochemical consequences of these activities with depth in iron mound sediments. Schwertmannite would transform into goethite as depth increases. Along with a Fe(II), pH, and FeRB increase with depth, while O_2, sulfate, and FeOB would all decrease with depth.

interface and increase with depth. Also, because FeRB activities would only occur at depth in O_2-depleted zones, the transformation to goethite would occur at a greater depth. Some of the results, such as, FeRB decreasing with depth and the FeOB abundances exhibiting homogeneity throughout, suggest that our conceptual model of distributions of microbial activities based on diffusion of O_2 may not be entirely accurate.

$$4\ Fe^{2+} + O_2 + 10\ H_2O \rightarrow 4\ Fe(OH)_3 + 8\ H^+ \quad \text{(Fe(II) oxidation) (eq. 4)}$$

$$CH_2O + 4\ Fe(OH)_3 + 8\ H^+ \rightarrow CO_2 + 4\ Fe^{2+} + 9\ H_2O \quad \text{(Fe(III) reduction) (eq. 5)}$$

$$2\ CH_2O + SO_4^{2-} + H^+ \rightarrow 2\ CO_2 + HS^- + 2\ H_2O \quad \text{(Sulfate reduction) (eq. 6)}$$

To understand what is occurring within the iron mound I will discuss the meaning of the results from the sediment-water interface to depth within the sediments. I hypothesized that if distribution of FeOB are dependent on vertical diffusion of O_2 within the sediments, it would be expected to see a higher concentration of FeOB on top. The hypothesis also states if there is a decrease in Fe(II) concentration, a slight decrease in sulfate concentration may occur due to incorporation of sulfate in Fe(III) hydroxysulfate phases (e.g. schwertmannite). This biogeochemical pattern is what I observed between the sediment-water interface and a depth of 2-3 cm (figure 4). At the sediment-water interface the Fe(II) was oxidized to Fe(III), with schwertmannite expected to be the initial product of this activity (Bertel et al., 2011). Sediments had a lower pH, lower pore-water concentration of Fe(II), and relatively high abundance of FeOB. At the sediment-water interface, there was also a higher sulfate concentration, which decreased slightly as depth increased. The removal of sulfate from solution as depth increases could be attributed to the incorporation into Fe(III) hydroxysulfate phases (Bigham et al., 1990; Burton et

al., 2007), as a consequence of microbiological Fe(II) oxidation near the sediment-water interface. Analysis of the solid phases by XRD suggested that the predominant mineral at shallower depth was a mixture of poorly crystalline Fe(III) phases and the predominant mineral at greater depth was a more crystalline form of goethite.

As depth increased from the sediment-water interface to a depth of 2-3 cm, the FeRB abundance increased, and the pore-water Fe(II) concentration increased due to the reductive dissolution of Fe(III) phases (e.g. schwertmannite) by FeRB activities (equation 7) (Burton et al., 2007). Anaerobic activities in iron mounds may lead to the reductive dissolution of Fe(III) hydroxides via the direct, enzymatic reduction of Fe(III) by Fe(III)-reducing bacteria (FeRB) (equation 5) or by reaction with sulfide produced by sulfate-reducing bacteria (SRB) (equation 6) (Ehrlich et al., 2009; Dvorak et al., 1992; Christensen et al., 1996).

$$CH_3COOH + Fe_8O_8(OH)_6(SO_4^{2-}) + 12\ H^+ \rightarrow 2HCO^{3-} + Fe^{2+} + SO_4^{2-} + 10\ H_2O \quad \text{(eq. 7)}$$

At a depth of 2 cm, the poorly crystalline Fe(III) phases were no longer stable and transformed into a more crystalline form of goethite, which was likely the final product of mineralogical transformations at the base of the deposits and induced by FeRB activities (Gagliano et al., 2004). From the sediment-water interface to a depth of 2-3 cm there was a slight decrease in FeOB abundance, and FeRB were the most abundant at this depth interval but O_2 was still present at this depth (Brantner et al., submitted). As such, this can be considered an aerobic zone, and it was hypothesized that Fe(III) reduction should only occur in an anaerobic zone. However, in AMD-impacted systems, the demarcation between aerobic and anaerobic metabolism appears to be nebulous. For instance, some Fe(III) reducing bacteria reduce Fe(III) hydroxides optimally under microaerobic conditions (Kusel et al., 2002; Malki et al., 2008) suggesting that aerobic Fe(II) oxidation

and Fe(III) reduction may occur in close proximity to each other. Several AMD-associated microorganisms are capable of both Fe(II) oxidation and Fe(III) reduction (Coupland et al., 2008). These results indicate that Fe(III) reduction may proceed under oxic conditions.

Continuing past the 2-3 cm depth, Fe(III) availability to FeRB was decreased by the development of more crystalline goethite (Bertel et al., 2012). This change in Fe(III) availability has been hypothesized to be a significant process influencing the switch from Fe(III) to sulfate reduction in anoxic acid-sulfate systems (Blodau, 2006; Burton et al., 2007). Goethite is also a less thermodynamically favorable TEA than poorly crystalline Fe(III) phases such as schwertmannite (Burton et al., 2007; Burton et al., 2008). The microbially mediated transformation of poorly crystalline Fe(III) phases to goethite would create a more recalcitrant goethite-associated pool of Fe(III) to support FeRB activity and consequently, enhance the stability of Fe(III) (Bertel et al., 2012). The transformation of poorly crystalline Fe(III) phases to less bioreducible goethite may explain the decreased abundances of FeRB in deeper iron mound sediments. Given this scenario, Fe(III) reduction may be a self-limiting process in the MF iron mound sediments, whereby reduction of schwertmannite-Fe(III) induces the formation of goethite, which is less susceptible to microbial reduction.

While FeRB decreased in abundance with increasing depth, FeOB abundances stayed constant, while there is a decrease in Fe(II) concentration in the 3-5 cm depth interval. While any decrease in Fe(II) concentration at varying depths could indicate oxidizing zones, it could also be a result of precipitation of FeS phases, or adsorption onto Fe(III) phases (Burton et al., 2008). After the initial reduction in sulfate concentration from the sediment-water interface until a depth of 2-3 cm, the sulfate concentration stayed relatively constant as it continued to depth. If sulfate reduction was occurring, the biogenic sulfide produced would be unlikely to accumulate and would have been

reoxidized by the surrounding Fe(III), not necessarily all the way to sulfate, but to some partially oxidized sulfur species (Neal et al., 2001; Poulton et al., 2004). Typically, black coloring in the sediment is indicative of sulfidogenesis. However, in this study, black coloring in the sediment was not observed so it is unlikely that the decrease in Fe(II) concentration is due to precipitation of Fe(II) as FeS. Extensive adsorption of Fe(II) onto Fe(III) phases at these depths is unlikely, since we observed a depletion of solid associated Fe(II) at depths below 2 cm in the MF iron mound sediments (Brantner et al., submitted).

It appears that the decrease in Fe(II) concentration is likely due to Fe(II) oxidation, but it occurred at depths where O_2 was not detected (Brantner et al., submitted). For Fe(II) oxidation to occur, aerobic Fe(II) oxidizing microbial communities must adapt to the continual burial within the Fe(III) hydroxides phases that they produce in order to transfer electrons from Fe(II) to O_2 that diffuses into AMD from the atmosphere. Conductive, microbially-produced nanowires that may extend millimeters from the bacteria towards a TEA were discovered in other systems that allow electrons to be transferred from cell to cell (Reguera et al., 2005). From a microbial perspective, far-afield extracellular transfer (EET) via electrically conductive nanowires may represent a common physiological strategy facilitating the transfer of electrons that could otherwise not be achieved under the physiochemical conditions in immediate proximity to individual cells. Abiotic far-afield electron transport has been suggested to occur in the terrestrial subsurface where (semi)conductive sulfide ore bodies facilitate the transfer of electrons from relatively deep, reducing strata to relatively shallow, oxidizing strata (Sato et al., 1960; Bigalke et al., 1997; Nielsen et al., 2010).

If far afield electron transfer occurs, I would expect to find a uniform distribution of FeOB. The results showed that the FeOB abundance stayed relatively uniform as depth increased, until an increase in abundance at 8 cm. While Fe(III) reduction occurred

in shallower sediments (as indicated by dissolved Fe(II) accumulation), after a depth of 2-3 cm the Fe(II) concentration decreased steadily. This suggests that EET may facilitate the transfer of electrons from Fe(II) in O_2-depleted regions of the iron mound to O_2 in shallower regions of the iron mound, and allows electrons to be transferred up to the O_2 through the Fe(III) hydroxide-rich sediment under anaerobic conditions (Meier et al., 2004). Some bacteria are capable of EET, thereby enabling them to use electron donors without direct cell contact with mineral phases or diffused O_2 (Nielsen et al., 2010). Furthermore, electrons conducted from microbial oxidation processes deep within the sediment may make a considerable contribution to supporting life in the subsurface sediment (Nielsen et al., 2010). It may also be possible that groundwater flow may transport O_2 to deeper sediments within the iron mound. However, the subsurface advection of O_2 is most likely minor, since depth-dependent depletion of O_2 has been observed in the iron mound (Brantner et al., submitted), and emergent AMD is anoxic before reaching the terrestrial surface (Gouin et al., 2012).

A common strategy for treatment of AMD is to divert AMD through limestone beds or channels (Cravotta and Trahan, 1999; Pennsylvania Department of Environmental Protection (PA-DEP), 1999; Nengovhela et al., 2004; Johnson and Hallberg, 2005). Limestone dissolution neutralizes acidic fluids, which subsequently removes Fe by precipitation of Fe(III) hydroxides (Cravotta and Trahan, 1999; Pennsylvania Department of Environmental Protection (PA-DEP), 1999; Johnson and Hallberg, 2005). This helps remove dissolved Fe(II), but these Fe(III) hydroxides coat limestone surfaces (referred to as ‘armoring’), which then limit further limestone dissolution and neutralization capacity (Pennsylvania Department of Environmental Protection (PA-DEP), 1999; Rose et al., 2004; Weaver et al., 2004). To limit armoring, systems like the iron mound might be constructed in which FeOB may remove Fe(II) from AMD. This Fe-free water may then be neutralized using limestone before it is released into nearby streams (Nengovhela et

al., 2004). However, if iron mounds are to be utilized for AMD treatment, the stability of the resultant Fe(III) phases must be addressed. For instance, extensive microbiological reduction of Fe(III) phases might lead to the "re-release" of Fe that had been previously immobilized within the iron mound. The results of the work described here indicate that while Fe(III) reduction occurs in shallower regions of the sediments, FeOB activity throughout the depth of the iron mound may serve to maintain the Fe(III) phases in an oxidized, and thus, a relatively insoluble form.

CHAPTER V

CONCLUSIONS

Mineralogical and geochemical gradients, along with distributions of microbial activities with depth within an acid mine drainage-derived iron mound were evaluated. Analysis of the solid phases was done by XRD, which indicated that poorly crystalline Fe(III) phases were transformed to more crystalline goethite phases with increasing depth in the sediments, though based on aqueous chemistry, sulfate was not released into solution when this occurred. Culture-dependent enumeration of FeOB indicated that abundances of those organisms were relatively constant to a depth of 9 cm. Culture-dependent enumeration of FeRB indicated the highest abundance of those organisms at a depth interval of 2-3 cm, which coincided with the maximal dissolved Fe(II) concentration. FeRB abundance subsequently decreased in abundance with increasing depth, which may be attributable to the poor bioreducibility of Fe(III) associated with goethite, which was the predominant Fe(III) phase detected in deeper sediments. After the 2-3 cm depth interval, Fe(II) concentrations decreased. It appears that the decrease in Fe(II) concentration is likely due to Fe(II) oxidation, but occurred at depths where O_2 is not likely to be detected. To allow anaerobic activities and oxidizing zones concurrently at depth, EET may be occurring. EET may facilitate the transfer of electrons that could otherwise not be achieved under the physiochemical conditions in immediate proximity to individual cells.

REFERENCES

Anderson RT, Lovley DR. (1997). Ecology and biogeochemistry of in situ groundwater bioremediation. Adv Microbial Ecol. 15:289-350.

Baker BJ, Banfield JF. (2003). Microbial communities in acid mine drainage. FEMS Microbial Ecol. 139-152.

Banks, D., Younger, P.L., Arnesen, R.T., Iversen, E.R. & Banks, S.B. (1997) Mine-water chemistry: the good, the bad and the ugly. Environmental Geology. 157-174

Berner, RA. (1969). Migration of iron and sulfur within anaerobic sediments during early diagenesis. Am. Jour. Sci. 19-42.

Bertel D, Peck J, Quick TJ, Senko JM. (2012). Iron transformations induced by an acid-tolerant Desulfosporosinus species. AEM. 81-88.

Bigalke J, Grabner EW. (1997). The geobattery model: A contribution to large-scale electrochemistry. Electrochim. Acta. 3443-3452.

Bingham JM, Schwertmann U, Carlson L, Murad E. (1990). A poorly crystallized oxyhydroxysulfate of iron formed by bacterial oxidation of Fe(II) in acid mine waters. Geochim Cosmochim Acta 54:2743-2758.

Bingham JM, Carlson L, Murad E. (1994). Schwertmannite, a new iron oxyhydroxysulfate from Pyhasalmi, Finland, and other localities. Miner. Mag. 58, 641-648.

Blodau, C. (2006). A review of acidity generation and consumption in acidic coal mine lakes and their watersheds. Sci. 307–332.

Borch T, Kretzschmar R, Kappler A, Cappellen PV, Ginder-Vogel M, Voegelin A,

Campbell K. (2009). Biogeochemical redox processes and their impact on contaminant dynamics. Environ. Sci. Technol. 15–23

Brantner JS, Haake ZJ, Burwick JE, Menge CM, Hotchkiss ST, Senko JM. (2014). Depth-dependent geochemical and microbiological gradients in Fe(III) deposits resulting from coal mine-derived acid mine drainage. Frontiers in Microbiology. Submitted.

Burton ED, Bush RT, Sullivan LA, Mitchell DRG. (2007). Reductive transformations of iron and sulfur in schwertmannite-rich accumulations associated with acidified coastal lowlands. Geochim. Cosmochim. Acta 71:4456 –4473.

Burton ED, Bush RT, Sullivan LA, Mitchell DRG. (2008). Schwertmannite transformation to goethite via the Fe(II) pathway: reaction rates and implications for iron-sulfide formation. Geochim. Cosmochim. Acta 72:4551-4564.

Champ DR, Gulens J, Jackson RE. (1979). Oxidation-reduction sequences in ground water flow systems. Can. J. Earth Sci., 16, 12-23.

Christensen NL, Bartuska LA, Brown JH, Carpenter S, D'Anotonio C, Francis R, Franklin JF, MacMahon JA, Noss RF, Parsons DJ, Peterson CH, Turner MG, Moodmansee RG. (1996). The report of the Ecological Society of America Committee on the scientific basis for ecosystem management. Ecological Applications. 6:665-691.

Christensen TH, Bjerg PL, Banwart SA, et al. (2000). Characterization of redox conditions in groundwater contaminant plumes. Journal of Contaminant Hydrology, 45, 165-241.

Coates JD, Achenbach LA. (2001). The biogeochemistry of aquifer systems. Manual of Environmental Microbiology, 2nd Edition, ASM Press, Washington, DC. 719-727.

Colmer AR, Hinkle ME. (1947). The role of microorganisms in acid mine drainage: a preliminary report. Science. 253-255.

Colwell RR. (1979). Enumeration of specific populations by the most-probable-number (MPN) method. Native Aquatic Bacteria: Enumeration, Activity, and Ecology, ASTM STP, J.W. Costerton and R.R. Colwell, Eds., American Society for Testing and Materials, 56-61.

Coupland K, Johnson DB. (2008). Evidence that the potential for dissimilatory ferric iron reduction is widespread among acidophillic heterotrophic bacteria. EMS Microbiol. Lett. 279:30-35.

Cravotta III CA, Trahan MK. (1999). Limestone drains to increase pH and remove dissolved metals from acidic mine drainage. Appl Geochem 14: 581-606.

DeSa TC, Brown JF, Burgos WD. 2010. Laboratory and field-scale evaluation of low-pH Fe(II) oxidation at Hughes Borehole, Portage, Pennsylvania. Mine Water Environ. 239–247.

Dvorak DH, Hedin RS, Edenborn HM & McIntire PE. (1992). Treatment of metal-contaminated water using bacterial sulfate reduction: Results from pilot-scale reactors. Biotechnol. Bioeng. 40: 609–616Ehrlich HL, Newman DK. (2009). Geomicrobiology. Boca Raton, FL: CRC Press.

Espana JS, Pastor ES, Pamo EL. (2013). Iron terraces in acid mine drainage systems: a discussion about the organic and inorganic factors involved in their formation through observations from the Tintillo acidic river (Riotinto Mine, Huelva, Spain). GES. 133-151.

Frazer L. (2001). Probing the depths of a solution for acid mine drainage. EHP J. 486-489.

Froelich, PN, Klinkhammer GP, Bender ML, Luedtke NA, Heath GR, Cullen D, Dauphin P, Hammond D, Hartman B, Maynard V. (1979). Early oxidation of organic matter in pleagic sediments of the eastern equatorial Atlantic: suboxic diagenesis. Geochem et Cosmochim. Acta. 1075-1090.

Gagliano WB, Brill MR, Bingham JM, Jones FS, Traina SJ. (2004). Chemistry and mineralogy of ochreous sediments in a constructed mne drainage wetland. Geochim Cosmochim Acta 68:2119-2128.

Gouin M, Saracusa E, Clemons CB, Senko J, Kreider KL, Young GW. (2013). A mathematical model of a passive scheme for acid mine drainage remediation. Int J Geomath. 4:27-53.

Groom CR, Allen FH. (2011). The Cambridge Structural Database: experimental three-dimensional information on small molecules is a vital resource for interdisciplinary research and learning. 1002

Hammack RW, Hedin RS. (2013). Microbial sulfate reduction for the treatment of acid mine drainage: a laboratory study. Pittsburgh research center. U.S. bureau of mines. U.S. Department of the Interior. Pittspurgh, PA.

Hansel CM, Benner SG, Neiss J, Dohnalkova A, Kukkadapu RK, Fendorf S. (2003). Secondary mineralization pathways induced by dissimilatory iron reduction of ferrihydrite under advective flow. Geochim. Cosmochim. Acta 67, 2977-2992.

Heguy DL, Nagl GJ. (2003). Consider optimized iron-redox processes to remove sulfur. GPC. 53-57.

Johnson DB. (1995). Selective solid media for isolating and enumerating acidophilic bacteria. J Microbiol Meth. 205-218.

Johnson DB, Hallberg KB. (2005). Acid mine drainage remediation options: a review. STE. 3-14

Kusel K, Roth U, Drake HL. (2002). Microbial reduction of Fe(III) in the presence of oxygen under low pH conditions. Environ. Microbiol. 4:414-421.

Lichvar L. (1997). Acid mine drainage. Fly Fisherman, 26.

Lovley DR, Phillips EJP. (1987). Rapid assay for microbially reducible ferric iron in aquatic sediments. Appl Environ Microbiol. 1536-1540.

Lovley DR, Phillips EJP. (1987). Competitive mechanisms for inhibition of sulfate reduction and methane production in the zone of ferric iron reduction in sediments. Appl. Environ. Microbiol. 1472-1480.

Lovley DR, Chapelle FH. (1995). Deep subsurface microbial processes. Rev Geophys. 33:365-381.

Lyngkilde J, Christensen TH. (1992). Redox zones of a landfill leachate pollution plume (Vejen, Denmark). J Contamin Hydrol. 10:273-289.

Malki M, De Lacey AL, Rodriguez N, Amils R, Fernandez VM. (2008). Preferential use of an anode as an electron acceptor by an acidophilic bacterium in the presence of oxygen. Applied Environmental Microbiology. 74:4472-4476.

Martin, S. T., Schlenker JC, Malinowski A, Hung H-M, and Rudich Y (2003), Crystallization of atmospheric sulfate-nitrate-ammonium particles, Geophys. Res. Lett., 30, 2102, doi:10.1029/2003GL017930, 21.

Martin ST. (2005). Precipitation and dissolution of iron and manganese oxides.

Environmental Catalyst. (V.H. Grassian, Ed), CRC Press: Boca Raton. 61-81

Meier J, Babenzien H-D, Wendt-Potthoff K. (2004). Microbial cycling of iron and sulfur in sediments of acidic and pH-neutral mining lakes in Lusatia (Brandenburg, Germany). Biogeochemistry. 135-156.

Mielke, R.E., Pace, D.L., Porter, T., and Southam, G. (2003). A critical stage in the formation of acid mine drainage: colonization of pyrite by Acidithiobacillus Ferrooxidans under pH-neutral conditions. Geobiology. 81–90.

Neal et al., (2001). Iron sulfides and sulfur species produced at hematite surfaces in the presence of sulfate-reducing bacteria. Geochim. Cosmochim. Acta 66:223-235.

Neculita CM, Zagury GJ, Bussiere B. (2007). Passive treatment of acid mine drainage in bioreactors using sulfate-reducing bacteria: critical review and research needs. JEQ 1-16.

Nengovhela NR, Strydom CA, Maree JP, Greben HA. (2004). Chemical and biological oxidation of iron in acid mine water. Mine Wat Environ 23: 76-80.

Newcombe CE, Brennan RA. (2010). Improved passive treatment of acid mine drainage in mushroom compost amended with crab-shell chitin. 616-626.

Nielsen LP, Risgaard-Petersen N, Fossing H, Christensen PB, Sayama M. 2010. Electric currents couple spatially separated biogeochemical processes in marine sediment. Nature. 1071-1074.

Peine A, Tritschler A, Kusel K, Peiffer S. (2000). Electron flow in an iron-rich acidic sediment – evidence for an acidity-drive iron cycle. Limnol. Oceanogr. 1077-1087.

Pennsylvania Department of Environmental Protection (PA-DEPP) (1999). The science of acid mine drainage and passive treatment. PA-DEP publication, Bureau of Abandoned Mine Reclamation, Harrisburg, PA.

Poulton SW, Krom MD, Raiswell R. (2004). A revised scheme for the reactivity of iron (oxyhydr)oxide minerals towards dissolved sulfide. Geochim. Cosmochim. Acta 68:3703–3715.

Reguera G, McCarthy KD, Mehta T, Nicoll JS, Tuominen MT, Lovley DR. (2005). Extracellular electron transfer via microbial nanowires. Nature. 1098-1101.

Revil A, Mendonca CA, Atekwana EA, Kulessa B, Hubbard SS, Bohlen KJ. 2010. Understanding biogeobatteries: where geophysics meets microbiology. J. Geophys. Res. G00G02.

Rose AW, Bisko D, Daniel A, Bower MA. (2004). An 'autopsy' of the failed Tangascootak #1 vertical flow pond. Proceedings of the National Meeting of the American Society of Mining and Reclamation and the 25th West Virginia Surface Mine Drainage Task Force. Published by ASMR, Lexington KY.

Sato, M, Mooney HM. (1960). The electrochemical mechanism of sulfide self-potentials. Geophysics. 25:226-249.

Senko JM, Bertel D, Quick TJ, Burgos WD. (2011). The influence of phototrophic biomass on Fe and S redox cycling in an acid mine drainage-impacted system. Mine Water Environ. 38-46.

Senko JM, Wangugi p, Lucas M, Bruns MA, Burgos WD. (2008). Characterization of Fe(II) oxidizing bacterial activities and communities at two acidic Appalachian coal mine drainage-impacted sites. ISME. 1134-1145

Senko JM, Zhang G, McDonough JT, Bruns MA, Burgos WD. (2009). Metal reduction at low pH by a Desulfosporosinus species: implications for the biological treatment of acid mind drainage. Geomicrobiol. 71-82.

Spalding BP, Brooks SC. (2005). Permeable environment leaching capsules (PELCAPs) for in situ evaluation of contaminant immobilization in soil. Environ. Sci. Technol. 8912-8918.

Stookey LL. (1970). Ferrozine-a new spectrophotometric reagent for iron. Anal. Chem. 42:779 -781.

Stumm W, Morgan JJ. (1996). Aquatic chemistry. Wiley-Interscience, Hoboken, New Jersey, USA.

Tanner RS. (1997). Cultivation of bacteria and fungi, p 52–60. InHurst CJ, Knudsen GR, McInerney MJ, Stetzenbach LD, Walter MV (ed), Manual of Environmental Microbiology. ASM Press, Washington, DC.

Weaver KR, Lagnese KM, Hedin RS. (2004). Technology and design advances in passive treatment system flushing. Proceedings of the National Meeting of the American Society of Mining and Reclamation and the 25th West Virginia Surface Mine Drainage Task Force. Published by ASMR, Lexington KY.

APPENDIX

RAW DATA

Depth Increment (cm)	pH	pH Standard Deviation	Pore-water Fe(II) (mM)	Fe(II) Standard Deviation
0.3	-	-	3.390	0.326
0.8	-	-	4.795	0.115
1	3.040	0.050	-	-
1.3	-	-	5.651	0.263
1.8	-	-	4.713	0.858
2	2.945	0.095	-	-
2.3	-	-	6.709	0.172
2.8	-	-	6.691	0.748
3	2.865	0.055	-	-
3.3	-	-	4.997	0.369
3.8	-	-	4.507	1.173
4	2.845	0.045	-	-
4.3	-	-	3.436	0.661
4.8	-	-	4.936	0.131
5	2.745	0.055	-	-
5.3	-	-	3.379	0.414
5.8	-	-	3.001	0.047
6	2.765	0.005	-	-
6.3	-	-	2.819	0.0
6.8	-	-	2.762	0.221
7	2.745	0.005	-	-
7.3	-	-	3.018	0.432
8	2.790	0.020	-	-
9	2.755	0.005	-	-
10	2.825	0.035	-	-

Depth Increment (cm)	Pore-water Sulfate (mM)	Sulfate Standard Deviation	FeRB (MPN/g)	FeOB (CFU/g)	FeOB Standard Deviation
0.3	127.127	138.161	-	-	-
0.8	112.111	116.664	-	-	-
1	-	-	6285.7140	5329.3413	538.9222
1.3	99.070	106.562	-	-	-
1.8	99.341	102.754	-	-	-
2	-	-	18750.0000	1768.9906	832.4662
2.3	85.777	89.420	-	-	-
2.8	85.356	90.008	-	-	-
3	-	-	3278.6890	1584.5070	176.0563
3.3	87.432	87.671	-	-	-
3.8	81.199	81.705	-	-	-
4	-	-	612.2449	1250.0000	220.5882
4.3	76.372	77.144	-	-	-
4.8	84.961	89.774	-	-	-
5	-	-	1271.1860	2028.5087	54.8246
5.3	79.449	79.782	-	-	-
5.8	76.762	78.145	-	-	-
6	-	-	710.5263	1802.3256	290.6977
6.3	74.749	76.080	-	-	-
6.8	79.705	86.337	-	-	-
7	-	-	148.5149	3011.3636	511.3636
7.3	75.749	78.210	-	-	-
8	-	-	308.8235	2270.5314	144.9275
9	-	-	22.3881	18281.5357	1919.5612
10	-	-	-	-	-